JAST, Vol. 5, No. 3, pp 129–138

JAST
Journal of Aerospace Science and Technology

Vibration Analysis of FGM Cylindrical Shells Under Various Boundary Conditions

R. Ansari[1], M. Darvizeh[2], M. Hemmatnezhad[3]

In this paper, a unified analytical approach is proposed to investigate the vibrational behavior of functionally graded shells. Theoretical formulation is established based on Sanders' thin shell theory. The modal forms are assumed to have the axial dependency in the form of Fourier series whose derivatives are legitimized using Stoke's transformation. The material properties are assumed to be graded in the thickness direction according to different volume fraction functions such as power-law, sigmoid, double-layered and exponential distributions. A FGM cylinderical shell made up of a mixture of ceramic and metal is considered. The Influence of some commonly used boundary conditions, the effect of changes in shell geometrical parameters and variations of volume fraction functions on the vibration characteristics are studied through comparing the results of the present theory with those of the First order Shear Deformation Theory (FSDT). Furthermore, the results obtained for a number of particular cases show good agreement with those available in the open literature. The simplicity and the capability of the present method are also discussed.

INTRODUCTION

Functionally graded materials (FGMs) have experienced considerable attention in many engineering applications since they were first introduced in 1984 in Japan [1, 2]. Covering a wide spectrum of functional operation principles and addressing a large variety of application fields, FGMs have been under worldwide development during recent years. They are now developed for general use as structural components in extremely high temperature environments such as rocket engine components, space plan body, nuclear reactor components, first wall of fusion reactor, engine components, turbine blades, hip implant and other engineering and technological applications. A detailed discussion of their design, processing and applications can be found in [3]. FGMs are also promising candidates for future intelligent composites [4]. They are multifunctional composite materials, and are microscopically inhomogeneous, wherein mechanical properties vary smoothly and continuously from one surface to another. The most well known FGM is compositionally graded from a ceramic to a metal to incorporate such diverse properties as heat, wear and oxidation resistance of ceramics with the toughness, strength, machinability and bending capability of metals. With the increased usage of these materials, it is important to understand the vibrating behaviors of FGM Cylindrical shells which have a vast range of applications in engineering and technology. A good overview of preliminary work has been given by Leissa [5]. There are also some good reviews on vibration of composite shell, which can be found in the literature [6-9]. Loy *et.al.* [10] analyzed the frequency spectrum of FGM cylindrical shells comprising of stainless steel and nickel with simply supported boundary conditions. It was found that the frequency characteristics are similar to those observed for homogeneous isotropic shells, and are altered by the constituent volume fractions and the configurations of the constituent material. Pradhan *et.al.* [11] studied vibration characteristics of a FGM cylindrical shell made up of stainless steel and zirconia for various boundary conditions. This analysis is carried out based on the Rayleigh-Ritz variational approach by applying the beamfunctions. In their study, the effects of boundary conditions and

1. *Assistant Professor, Dept. of Mech. Eng., Guilan Univ., Rasht, Iran.*
2. *Professor, Dept. of Mech. Eng., Guilan Univ., Rasht, Iran.*
3. *M.Sc. Student, Dept. of Mech. Eng., Guilan Univ., Rasht, Iran.*

volume fractions on the shell frequencies are studied. Naeem [12] employs a polynomial based Rayleigh-Ritz approach in order to investigate natural frequencies of FGM cylindrical shells for various boundary conditions. In their analysis, equations are formulated by Sanders thin-shell theory. Patel *et.al.* [13] analyses free vibration of FGM elliptical cylindrical shells using Finite Element Method (FEM) based on Higher order Shear Deformation Theory (HSDT). Ansari and Darvizeh [14] propose a novel unified exact approach for investigating the vibrational behavior of FGM shells under arbitrary boundary conditions. In that work, theoretical formulation used were based on the first order shear deformation theory (FSDT). The present paper, which is related to the authors' previous work, deals with free vibration of FGM shells under various boundary conditions based on Sanders's shell theory. The aim of this investigation is to propose a simpler but still more accurate method than the authors' previous work capable of predicting the natural frequencies of FGM shells under various boundary conditions. The influence of some commonly used boundary conditions as well as different volume fraction functions of the constituent materials on the vibration characteristics are studied.

EQUATIONS OF MOTION

Consider a cylindrical shell made of FGM with a cross-sectional view as shown in Figure 1. Its geometrical parameters are described by R, the radius of the shell middle surface, and h, the thickness of the shell. The

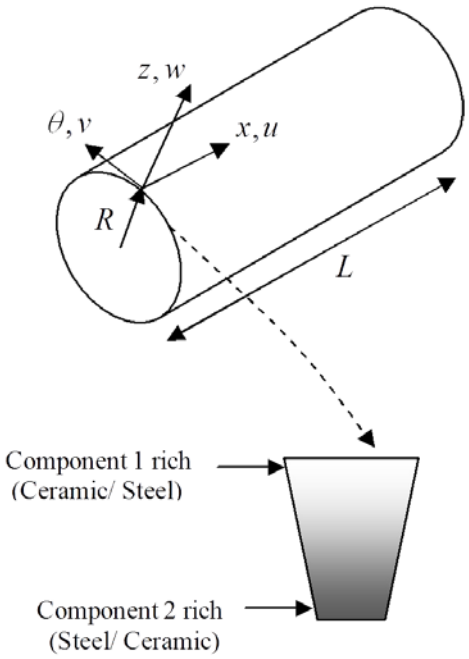

Figure 1. An element of a FGM shell.

Sanders-type shell equations are used [15].

$$RN_{x,x} + N_{x\theta,\theta} = RI_1\ddot{u}$$

$$RN_{x\theta,x} + N_{\theta\theta,\theta} + \frac{1}{R}M_{\theta\theta,\theta} + M_{x\theta,x} = RI_1\ddot{v}$$

$$RM_{x,xx} + 2M_{x\theta,x\theta} + \frac{1}{R}M_{\theta,\theta\theta} - N_\theta = RI_1\ddot{w} \tag{1}$$

where R is the radius of the shell, N and M are the resultant forces and moments defined thereafter and I_1 is the inertia term for FGM shell defined as:

$$I_1 = \int_{-\frac{h}{2}}^{\frac{h}{2}} \rho(z)dz \tag{2}$$

Here h is the thickness of the shell. Natural and geometric boundary conditions at the ends of the cylindrical shell have a combination like the following:

$$\left\{\begin{array}{llll} N_x = 0 & \text{or} & u = 0, \\ N_{x\theta} = 0 & \text{or} & v = 0, \\ Q_x = 0 & \text{or} & w = 0, \\ M_x = 0 & \text{or} & \frac{\partial w}{\partial x} = 0. \end{array}\right\} \tag{3}$$

Here:

$$Q_x = \partial M_x/\partial x + (2/R)\partial M_{x\theta}/\partial\theta \tag{4}$$

STRESS RESULTANT – STRAIN RELATIONS

The relationships between boundary forces and strains for a cylinderical shell are given as:

$$\left\{\begin{array}{c} N_x \\ N_\theta \\ N_{x\theta} \\ M_x \\ M_\theta \\ M_{x\theta} \end{array}\right\} = \left[\begin{array}{cccccc} A_{11} & A_{12} & 0 & B_{11} & B_{12} & 0 \\ A_{12} & A_{22} & 0 & B_{12} & B_{22} & 0 \\ 0 & 0 & A_{66} & 0 & 0 & B_{66} \\ B_{11} & B_{12} & 0 & D_{11} & D_{12} & 0 \\ B_{12} & B_{22} & 0 & D_{12} & D_{22} & 0 \\ 0 & 0 & B_{66} & 0 & 0 & D_{66} \end{array}\right] \left\{\begin{array}{c} \varepsilon_x \\ \varepsilon_\theta \\ \gamma_{x\theta} \\ K_x \\ K_\theta \\ K_{x\theta} \end{array}\right\} \tag{5}$$

where A_{ij}, B_{ij} and D_{ij} are the stiffnesses of the FGM shell as:

$$(A_{ij},\, B_{ij},\, D_{ij}) = \int_{-\frac{h}{2}}^{\frac{h}{2}} Q_{ij}(1,\, z,\, z^2)dz \tag{6}$$

here Q_{ij}, denote the plane stress-reduced stiffnesses in the principal coordinate directions as:

$$Q_{11} = Q_{22} = \frac{E(z)}{1-\upsilon^2}$$

$$Q_{12} = \frac{\upsilon(z)E(z)}{1-\upsilon(z)^2}$$

$$Q_{44} = Q_{55} = Q_{66} = \frac{E(z)}{2\,(1+\upsilon(z))} \tag{7}$$

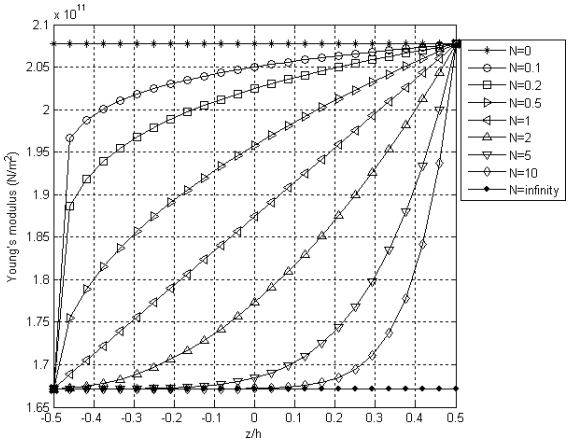

Figure 2. Young's modulus variation associated with different power law exponents for a power-law FGM shell.

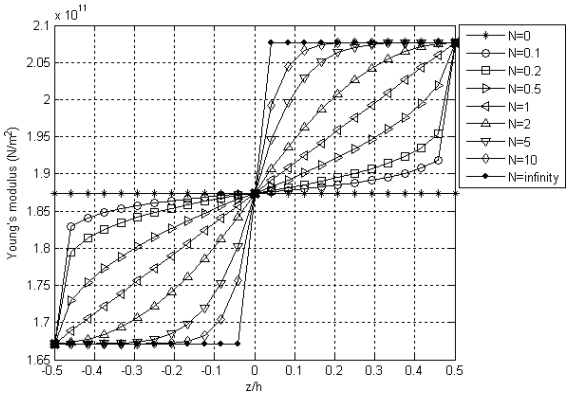

Figure 3. Young's modulus variation associated with different exponent indexes for a sigmoid FGM shell.

FUNCTIONALLY GRADED SHELLS

Consider the case of an FGM shell made up of a mixture of ceramic and metal. The material properties vary continuously across the thickness based on the following relations:

$$\begin{aligned} E(z) &= E_m + E_{cm}V_f(z), & E_{cm} &= E_c - E_m \\ \nu(z) &= \nu_m + \nu_{cm}V_f(z), & \nu_{cm} &= \nu_c - \nu_m \\ \rho(z) &= \rho_m + \rho_{cm}V_f(z), & \rho_{cm} &= \rho_c - \rho_m \end{aligned} \tag{8}$$

where subscripts m and c refer to the properties of metal and ceramic respectively, and $V_f(z)$ can be defined by different functions as follows:

For power-law FGMs:

$$V_f(z) = \left(\frac{z}{h} + \frac{1}{2}\right)^N \tag{9}$$

where N is the material index, which indicates the material variation profile through the shell thickness. The variation of Young's modulus against the thickness for power-law FGM is depicted in Figure 2. As can be seen, $N = 0$ and $N = \infty$ refer to isotropic shells made of ceramic and metal respectively.

For sigmoid FGMs:

$$V_f(z) = \begin{cases} 1 - \frac{1}{2}\left(1 - \frac{2z}{h}\right)^N & 0 \le z \le \frac{h}{2} \\ \frac{1}{2}\left(1 + \frac{2z}{h}\right)^N & -\frac{h}{2} \le z \le 0 \end{cases} \tag{10}$$

Similarly, N designates the material variation profile across the thickness, whose role in Young's modulus alteration is shown in Figure 3. Here, $N = 0$ refers to an isotropic shell with the average properties of its constituent materials. Whereas, $N = \infty$ refers to a shell, half of the thickness of which is made of ceramic and the other half, of metal.

For double layered FGMs:

$$V_f(z) = \begin{cases} \left(1 - \frac{2z}{h}\right)^N & 0 \le z \le \frac{h}{2} \\ \left(1 + \frac{2z}{h}\right)^N & -\frac{h}{2} \le z \le 0 \end{cases} \tag{11}$$

as can be seen from Figure 4, the variation of Young's modulus in the thickness direction for a double layered FGM is perfectly symmetric at about $z = 0$ as expected.

For exponential FGMs [15, 16]:

$$\begin{aligned} E(z) &= E_m\, e^{\left(\frac{1}{h}\ln\frac{E_c}{E_m}\right)\left(z+\frac{h}{2}\right)} \\ v(z) &= v_m\, e^{\left(\frac{1}{h}\ln\frac{v_c}{v_m}\right)\left(z+\frac{h}{2}\right)} \\ \rho(z) &= \rho_m\, e^{\left(\frac{1}{h}\ln\frac{\rho_c}{\rho_m}\right)\left(z+\frac{h}{2}\right)} \end{aligned} \tag{12}$$

The Young's modulus variation across the thickness of a FGM shell with the exponential volume fraction function is drawn in Figure 5. Further on, FGM shells are assumed to have power-law volume fraction distribution, Eq. (9), unless it is mentioned so elsewhere. A typical material property P_i which is a function of the temperature, is given by [17]:

$$P_i = P_0\left(P_{-1}T^{-1} + 1 + P_1T + P_2T^2 + P_3T^3\right) \tag{13}$$

where $P_i(i = 0.3)$ are unique constants for each of the constituent materials.

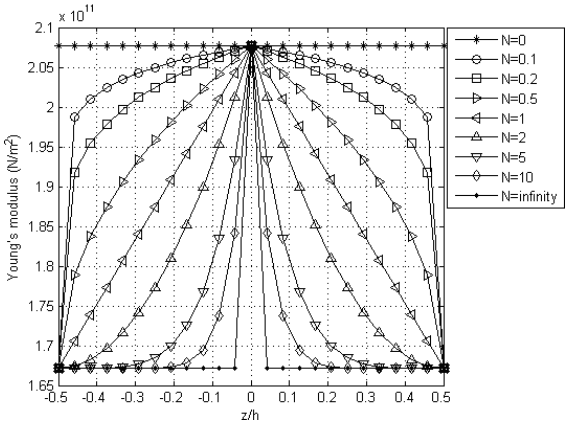

Figure 4. Young's modulus variation associated with different exponent indexes for a double layered FGM shell.

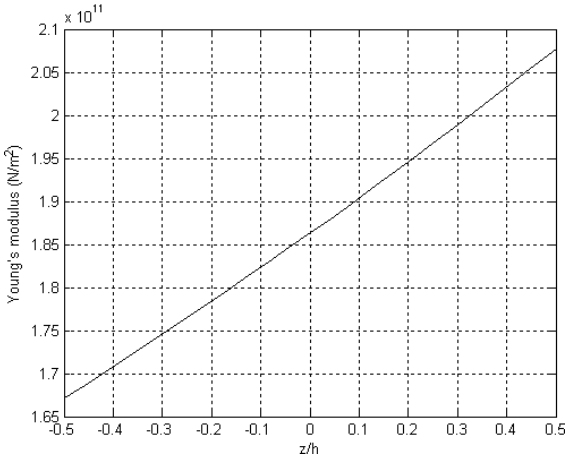

Figure 5. Young's modulus variation in the thickness direction for an exponential FGM shell.

FIELD EQUATIONS

Utilizing Eq. (5), Eq. (1) can be expressed in terms of displacement field and its corresponding derivatives as:

$$R[A_{11}u_{,xx} + \frac{A_{12}}{R}(v_{,x\theta} + w_{,x}) - B_{11}w_{,xxx} + \frac{B_{12}}{R^2}(v_{,x\theta} - w_{,x\theta\theta})] + A_{66}(v_{,x\theta} + \frac{1}{R}u_{,\theta\theta}) + \frac{B_{66}}{2R}(v_{,x\theta} - 2w_{,x\theta\theta}) = RI_1\ddot{u} \quad (14a)$$

$$R[A_{66}(v_{,xx} + \frac{1}{R}u_{,\theta x}) + \frac{B_{66}}{2R}(v_{,xx} - 2w_{,xx\theta})] + A_{12}u_{,x\theta} + \frac{A_{22}}{R}(v_{,\theta\theta} + w_{,\theta}) - B_{12}w_{,xx\theta} + \frac{B_{22}}{R^2}(v_{,\theta\theta} - w_{,\theta\theta\theta}) + \frac{1}{R}[B_{12}u_{,x\theta} + \frac{B_{22}}{R}(v_{,\theta\theta} + w_{,\theta}) - D_{12}w_{,xx\theta} + \frac{D_{22}}{R^2}(v_{,\theta\theta} - w_{,\theta\theta\theta})] + B_{66}(v_{,xx} + \frac{1}{R}u_{,x\theta}) + \frac{D_{66}}{2R}(v_{,xx} - 2w_{,xx\theta}) = RI_1\ddot{v} \quad (14b)$$

$$R[B_{11}u_{,xxx} + \frac{B_{12}}{R}(v_{,xx\theta} + w_{,xx}) - D_{11}w_{,xxxx} + \frac{D_{12}}{R^2}(v_{,xx\theta} - w_{,xx\theta\theta})] + 2B_{66}(v_{,xx\theta} + \frac{1}{R}u_{,xx\theta}) + \frac{D_{66}}{R}(v_{,xx\theta} - 2w_{,xx\theta\theta}) + \frac{1}{R}[B_{12}u_{,x\theta\theta} + \frac{B_{22}}{R}(v_{,\theta\theta\theta} + w_{,\theta\theta}) - D_{12}w_{,xx\theta\theta} - \frac{D_{22}}{R^2}(w_{,\theta\theta\theta\theta} - v_{,\theta\theta\theta})] - [A_{12}u_{,x} + \frac{A_{22}}{R}(v_{,\theta} + w) - B_{12}w_{,xx} + \frac{B_{22}}{R^2}(v_{,\theta} - w_{,\theta\theta})] = RI_1\ddot{w} \quad (14c)$$

MODAL FUNCTIONS

For a circular cylinderical shell, the displacement field can be written in the following form for any circumferential wave number n:

$$u(x,\,\theta,\,t) = \Psi_u(x)\cos n\theta \sin\omega t$$

$$v(x,\,\theta,\,t) = \Psi_v(x)\sin n\theta \sin\omega t$$

$$w(x,\,\theta,\,t) = \Psi_w(x)\cos n\theta \sin\omega t \quad (15)$$

Here Ψ_u, Ψ_v and Ψ_w are the modal functions corresponding to axial, tangential and radial displacements, respectively. The crucial part of the present analysis involves choosing appropriate series forms for these modal functions. The series should be simple in form while preserving orthogonality properties at the same time. It is not necessary that the series satisfy any particular boundary condition since we are seeking a general solution. There are two convenient sets of the Fourier series that meet all these requirements for the modal functions along the axial direction. The first set, designated as "CSS", where c and s stand for cos and sin respectively, is of the form:

$$\Psi_u(x) = A_{0n} + \sum_{m=1}^{\infty} A_{mn}\cos(m\pi x/L)$$

$$\Psi_v(x) = \sum_{m=1}^{\infty} B_{mn}\sin(m\pi x/L)$$

$$\Psi_w(x) = \sum_{m=1}^{\infty} C_{mn}\sin(m\pi x/L) \quad (16)$$

while the second set, designated as "SCC", can be written as:

$$\Psi_u(x) = \sum_{m=1}^{\infty} A_{mn} \sin(m\pi x/L)$$

$$\Psi_v(x) = B_{0n} + \sum_{m=1}^{\infty} B_{mn} \cos(m\pi x/L)$$

$$\Psi_w(x) = C_{0n} + \sum_{m=1}^{\infty} C_{mn} \cos(m\pi x/L) \tag{17}$$

The first set fulfills the exact solution for the shell with Simply supported ends with no Axial constraint (SNA-SNA), which has boundary conditions at each end of the form:

$$N_x = 0, \quad v = 0, \quad w = 0, \quad M_x = 0. \tag{18}$$

It is clear that sine series always give zero values at the end points unless one specifies the affected terms as:

$$\Psi_v(0) = v_0, \qquad \Psi_w(0) = w_0,$$
$$\Psi_v(L) = v_L, \qquad \Psi_w(L) = w_L. \tag{19}$$

These end values are required when Stoke's transformation is used to differentiate the displacement functions [18-20]. To maximize the generality of the formulation, a shell with Freely Supported ends with No Tangential constraint (FSNT) is chosen as a base problem for the set (CSS). The boundary conditions for such a shell is given by:

$$u = N_{x\theta} = Q_x = \frac{\partial w}{\partial x} = 0, \qquad (x = 0, L) \tag{20}$$

None of the ten boundary conditions given by Eq. (20) are satisfied by the CSS set, Eq. (16), on a term-by-term basis. Therefore, Stoke's transformation (see Appendix A) is now used to enforce constraints to satisfy the boundary conditions. This results in a general eigenvalue problem which can be used for any possible combination of boundary condition.

GENERAL FORMULATIONS

The substitution of the set of displacement functions and their derivatives into Eqs. (14a) to (14c), leads to an explicit relation for A_{0n} and a matrix equation in which A_{mn}, B_{mn} and O_{mn} are coupled together.

$$\left\{ \begin{bmatrix} K_{11} & K_{12} & K_{13} \\ & K_{22} & K_{23} \\ \text{Symm.} & & K_{33} \end{bmatrix} - \begin{bmatrix} I_1 & 0 & 0 \\ 0 & I_1 & 0 \\ 0 & 0 & I_1 \end{bmatrix} \omega^2 \right\} \begin{bmatrix} A_{mn} \\ B_{mn} \\ C_{mn} \end{bmatrix} = \begin{bmatrix} F_1 \\ F_2 \\ F_3 \end{bmatrix} \tag{21}$$

and

$$\left(K_{01} - I_1\omega^2\right) A_{0n} = F_{01} \tag{22}$$

where $K_{ij}(i, j = 1, 2, 3), K_{01}$ given in Appendix B, depends upon the material properties, the geometrical properties and the circumferential and axial mode numbers. In Eqs. (21) and (22) F_1 to F_3 and F_{01} are in terms of unknown end values, defined as:

$$\begin{aligned} F_1 &= f_1(\bar{u}_0 + \bar{u}_L(-1)^m) + f_2(v_0 + v_L(-1)^m) \\ &\quad + f_3(w_0 + w_L(-1)^m) + f_4(\bar{\bar{w}}_0 + \bar{\bar{w}}_L(-1)^m) \\ F_2 &= f_5(v_0 + v_L(-1)^m) + f_6(w_0 + w_L(-1)^m) \\ F_3 &= f_7(v_0 + v_L(-1)^m) + f_8(w_0 + w_L(-1)^m) \\ &\quad + f_9(\bar{\bar{w}}_0 + \bar{\bar{w}}_L(-1)^m) \end{aligned} \tag{23}$$

and

$$\begin{aligned} F_{01} &= f_{10}(\bar{u}_0 + \bar{u}_L(-1)^m) + f_{11}(v_0 + v_L(-1)^m) \\ &\quad + f_{12}(w_0 + w_L(-1)^m) + f_{13}(\bar{\bar{w}}_0 + \bar{\bar{w}}_L(-1)^m) \end{aligned} \tag{24}$$

In the above equations f_1 to f_{18} are given as:

$$f_1 = RA_{11}(\frac{\pi}{L})^2, \quad f_2 = \left[A_{12} + \frac{B_{12}}{R} + A_{66} + \frac{B_{66}}{2R}\right](\frac{n\pi}{L})$$

$$f_3 = A_{12}\frac{\pi}{L} + RB_{11}m^2(\frac{\pi}{L})^3 - (\frac{n^2\pi}{RL})(B_{12} - B_{66})$$

$$f_4 = -RB_{11}(\frac{\pi}{L})^3, \; f_5 = -(RA_{66} + \frac{3B_{66}}{2} + \frac{D_{66}}{2R})m(\frac{\pi}{L})^2$$

$$f_6 = -(B_{66} + B_{12} + \frac{D_{12}}{R} + \frac{D_{66}}{R})mn(\frac{\pi}{L})^2$$

$$f_7 = -(2B_{66} + B_{12} + \frac{D_{12}}{R} + \frac{D_{66}}{R})mn(\frac{\pi}{L})^2$$

$$f_8 = -(2B_{12}m(\frac{\pi}{L})^2 + RD_{11}m^3(\frac{\pi}{L})^4 + 2\frac{(D_{12}+D_{66})}{R}m \times (\frac{n\pi}{L})^2), \quad f_9 = RD_{11}m(\frac{\pi}{L})^4, \quad f_{10} = \frac{1}{2}RA_{11}\left(\frac{\pi}{L}\right)^2$$

$$f_{11} = \frac{1}{2}(A_{12} + \frac{B_{12}}{R} + A_{66} + \frac{B_{66}}{2R})$$

$$f_{12} = \frac{1}{2}\left[A_{12}\frac{\pi}{L} - \frac{B_{12}}{R}(\frac{n^2\pi}{L}) + \frac{B_{66}}{R}(\frac{n^2\pi}{L})\right]$$

$$f_{13} = -\frac{1}{2}RB_{11}\left(\frac{\pi}{L}\right)^3 \tag{25}$$

and the other four quantities, $\bar{u}_0, \bar{u}_L, \bar{\bar{w}}_L$ and $\bar{\bar{w}}_L$, are associated with the unspecified end forces N_x and moments M_x at the shell ends. Using Eqs. (21) and (22), A_{mn}, B_{mn}, C_{mn} and A_{0n} can now be expressed explicitly in terms of the eight unspecified boundary values $N_x^0, N_x^L, M_x^0, M_x^L, v_0, v_L, w_0, w_L$. As mentioned before, none of the eight boundary conditions of "FSNT" shells as given by Eq. (20) are satisfied by the assumed modal displacement forms in Eq. (16) on a term-by-term basis. Hence, it is necessary to enforce these

boundary conditions, which are both geometrical and natural in type. The geometric boundary conditions that must be imposed are associated with u and $\frac{\partial w}{\partial x}$. The natural boundary conditions that must be enforced are also associated with $N_{x\theta} = 0$ and $Q_x = 0$ at both ends with Q_x defined in Eq. (4). Substituting the Fourier coefficients given by Eqs. (21) and (22) into the eight constraint condition due to the geometric and natural boundary conditions, leads to the following homogeneous matrix equation.

$$[e_{ij}] \begin{bmatrix} N_x^0 \\ N_x^L \\ M_x^0 \\ M_x^L \\ v_0 \\ v_L \\ w_0 \\ w_L \end{bmatrix} = [0], \qquad (i,j = 1,2,...,8) \tag{26}$$

For a nontrivial solution of Eq. (26), the determinant of the coefficient matrix must vanish:

$$|e_{ij}| = 0, \qquad (i,j = 1,2,...,8) \tag{27}$$

resulting in a characteristic equation whose eigenvalues are the natural frequencies of the FSNT shell. The corresponding eigenvectors also determine the mode shapes. Each element of this frequency determinant is an infinite series. It should be pointed out that this frequency determinant is based on the exact satisfaction of the boundary conditions, and it can not only be used for the FSNT shells, but can also be employed to achieve the characteristic equation required for shells with arbitrary end conditions. Solutions for shells with other boundary conditions lead to a smaller size determinant than for the FSNT shell.

IMPOSING THE BOUNDARY CONDITIONS

To derive the appropriate characteristic equation of a specified boundary condition, the general matrix Eq. (26) must be tailored. To show how, the frequency determinant for clamped-free boundary condition is derived in this section. For this non-symmetric set of boundary conditions, we have:

$$u = v = w = \frac{\partial w}{\partial x} = 0, \qquad at\ x = 0$$

$$N_x = N_{x\theta} = Q_x = M_x = 0, \qquad at\ x = L \tag{28}$$

To enforce the geometric boundary conditions $u = 0$ and $\partial w/\partial x = 0$ at $x = 0$, one must allow the corresponding natural conditions N_x and M_x to take any non-zero value, respectively. In a similar manner, to impose the natural conditions $N_{x\theta} = 0, Q_x = 0$ at $x = L$, the geometrical boundary conditions v, w must also be released to have any value. Therefore without going through the direct procedure required to formulate the eigenvalue problem corresponding to this boundary condition, retaining the rows and columns in Eq. (26) associated with N_x^0, M_x^0, v_L, w_L leads to the following matrix equation for a clamped-free boundary condition:

$$[e_{ij}] \left[N_x^0 \ M_x^0 \ v_L \ w_L\right]^T = [0], \qquad (i,j = 1,3,6,8) \tag{29}$$

Similarly, the characteristic equation required for any other specified boundary condition can be extracted by tailoring Eq. (26) in an appropriate way.

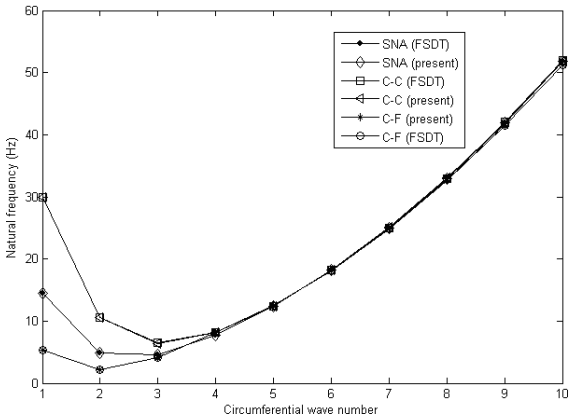

Figure 6. Frequency variation associated with different boundary conditions for a FGM shell.

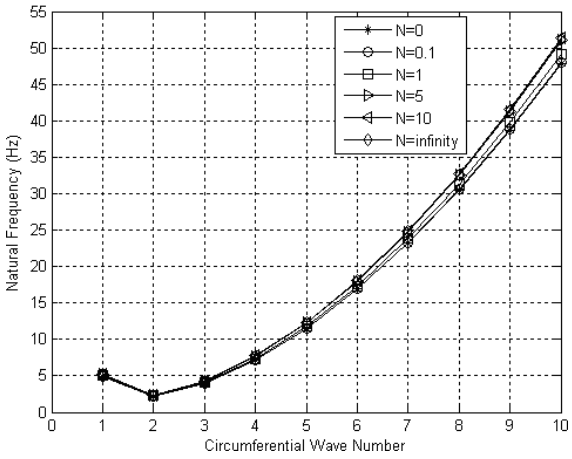

Figure 7. Frequency variation associated with different power law exponents for a clamped-free FGM shell.

MATERIAL PROPERTIES OF FGM

The constituent materials considered here are stainless steel and zirconia with the properties listed in Table 1 [11].

RESULTS AND DISCUSSION

The comparison of the results from the present analysis and those reported by [22, 23] is given in Table 2.

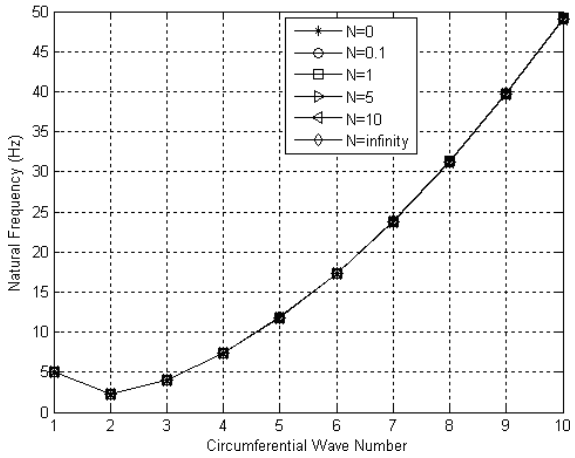

Figure 8. Frequency variation associated with different exponent indexes for a clamped-free sigmoid FGM shell.

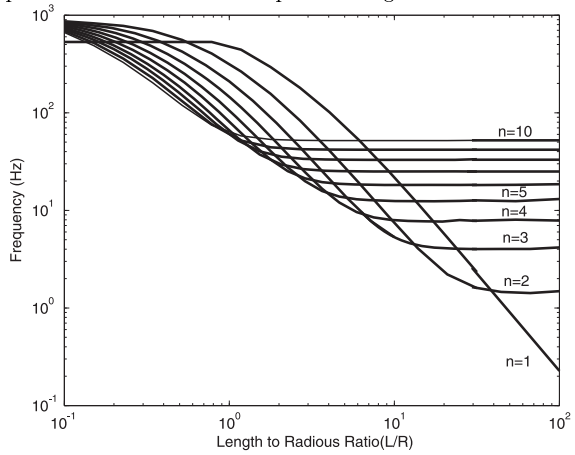

Figure 9. Frequency variation against the length-to-radius ratio of a Clamped-Free FGM shell ($h/R = 0.002$).

The shell considered here is an isotropic cylinder with clamped-free ends. Good agreement is achieved, which shows the capability of the present method in predicting natural frequencies of the cylindrical shells. Figure 6 illustrates the influence of the boundary conditions on the natural frequencies of the FGM shells. The boundary conditions considered here are SNA-SNA, Clamped-Clamped (C-C) and Clamped-Free (C-F) boundary conditions. The material properties used are those given in Table 1 at room temperature with shell parameters as $h/R = 0.002$, $L/R = 20$. The results show excellent agreement with those from FSDT. Figure 7 represents the natural frequencies of the power-law FGM shell with a clamped-free boundary condition versus circumferential mode numbers for the different power-law exponents N and $h/R = 0.002$, $L/R = 20$. The results obtained include pure stainless steel and pure zirconia shells corresponding to $N = 0$ and $N = \infty$, respectively. It is interesting to mention that for any other value of N, the frequency curve lies within the frequencies of the two extreme values of N, which belong to pure stainless steel and pure zirconia shells. In other words, alteration of the natural frequency of a FGM shell is easily achievable by varying the volume fraction of its constituent materials. Similar figure for a sigmoid FGM shell is also illustrated in Figure 8. As can be seen, the dependency of frequencies on power law exponents for the sigmoid FGM shell is not as much significant as those of power-law FGM. Figure 9 shows Frequency variation against the length-to-radius ratio of a clamped-free FGM shell. The variation of natural frequencies of a SNA-SNA FGM shell against the length-to-radius ratio is also illustrated in Figure 10. It is seen that, as the shell aspect ratio increases, the natural frequencies tend to decrease. Figure 11 shows the first mode shape of a clamped-free FGM shell as would be expected.

Table 1. Mechanical properties of constituent materials for FGM shells.

	Stainless Steel		Zirconia	
	E(Nm^{-2})	ν	E(Nm^{-2})	ν
P_{-1}	0	0	0	0
P_0	201.04E9	0.3262	244.27E9	0.288
P_1	3.08E-4	-2E-4	-1.371E-3	1.13E-4
P_2	-6.53E-7	3.8E-7	1.21E-6	0
P_3	0	0	-3.68E-10	0
ρ	8166 (Kgm^{-3})		5700 (Kgm^{-3})	

CONCLUSION

A general and unified exact solution procedure has been presented to investigate the vibrational behavior of FGM cylindrical shells under different boundary conditions. The advantage of the present method is to keep the complexity at a considerably low level yielding simplification in formulation without any loss of accuracy. Material properties are assumed to be temperature-dependent with gradient in the thickness direction of the shell. This gradient varies according to different volume fraction distributions including power-law, sigmoid, double-layered and exponential distributions. A FGM cylindrical shell made up of a mixture of ceramic and metal is considered. The

Table 2. Comparison of natural frequencies (Hz) for an isotropic cylinder with clamped-free ends ($L = 625.5$ mm, $R = 242.3$ mm, $h = 0.648$ mm, $E = 68.95$ GN/m^2, $\nu = 0.315$, $\rho = 2714.5$ kg/m^3).

n	Experimental Ref. [22]	Analytical Ref. [23]	Present method
2	-	333.9	328.18
3	155 and 157	175.5	174.90
4	107	111.7	111.91
5	89 and 91	94.2	94.28
6	102	105.8	105.57
7	130	134.0	133.40
8	166	171.7	170.81
9	208	216.4	215.13
10	260	267.0	265.41

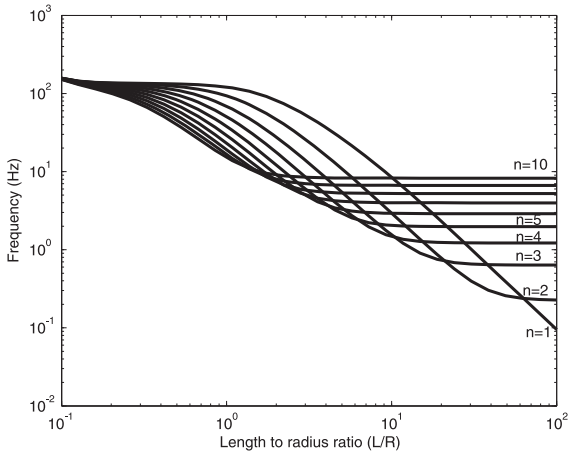

Figure 10. Frequency variation against the length-to-radius ratio of a SNA-SNA FGM shell ($h/R = 0.002$).

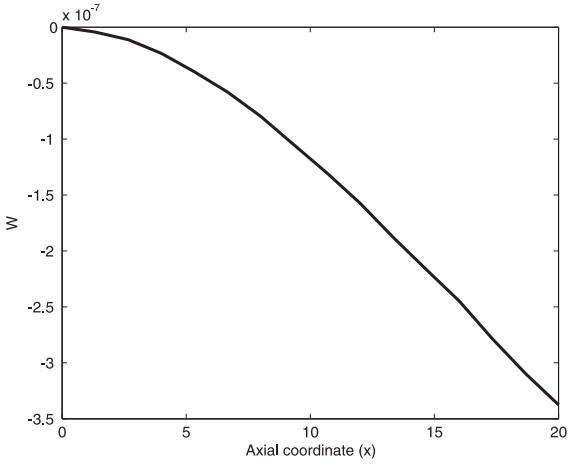

Figure 11. Mode shape associated with clamped-free boundary condition for a power-law FGM shell ($n = 1$, $L/R = 20$, $h/R = 0.002$).

frequency pattern of FGM shells is shown to be similar to those made from isotropic materials. Furthermore, the frequency curves associated with different values of the power law exponents, N, lie within the frequencies of the two extreme values of N, which belong to pure stainless steel and pure zirconia shells. This means that alteration of the natural frequency of a FGM shell is easily viable by varying the volume fraction of its constituent materials. The dependency of shell frequencies on exponent index in power-law FGMs is more significant compared to those of sigmoid FGMs. As one travels through the end conditions of SNA-SNA to fully clamped end condition, denoted by C-C, the influence of the boundary conditions is shown to increase the natural frequencies. This effect is more significant for lower values of circumferential wave numbers. However, for higher values, the effect of the changes in the boundary conditions diminishes such that the corresponding natural frequencies are found to coincide.

APPENDIX A: STOKES' TRANSFORMATION

Consider a function $f(x)$ represented by a Fourier sine series in the open range $0 < x < L$ and by values f_0 and f_L at the end points:

$$f(x) = \sum_{n=1}^{\infty} a_n \sin \frac{n\pi x}{L}, \qquad 0 < x < L,$$

$$f(0) = f_0, \quad f(L) = f_L,$$

Since it is not certain that the derivative $f'(x)$ can be represented by term-by-term differentiation of the sine series, the derivative is instead represented by an independent cosine series of the following form:

$$f'(x) = b_0 + \sum_{n=1}^{\infty} b_n \cos \frac{n\pi x}{L}$$

Stokes' transformation includes integrating by parts in the basic definitions of the coefficients to obtain the relationship between b_n and a_n as follows:

$$b_n = \frac{2}{L}\int_0^L f'(x)\cos\frac{n\pi x}{L}\mathrm{d}x = \frac{2}{L}\left[f(x)\cos\frac{n\pi x}{L}\right]_0^L$$

$$+ \frac{2n\pi}{L^2}\int_0^L f(x)\sin\frac{n\pi x}{L}\mathrm{d}x = \frac{2}{L}\left[(-1)^n f_L - f_0\right] + \frac{n\pi x}{L}a_n$$

Similar care must be taken when finding the correct sine series corresponding to $f''(x)$. Therefore, the complete set of derivative formulas for the sine series can be written as:

$$\begin{cases} f(x) = \sum\limits_{n=1}^{\infty} a_n \sin\frac{n\pi x}{L} & 0 < x < L, \\ f(0) = f_0, & f(L) = f_L, \end{cases}$$

$$\begin{cases} f'(x) = \frac{f_L - f_0}{L} - \sum\limits_{n=1}^{\infty}\left[\frac{2}{L}\left\{f_0 - (-1)^n f_L\right\} - \frac{\pi}{L}n a_n\right] \\ \qquad \times \cos\frac{n\pi x}{L}, \qquad 0 \le x \le L \end{cases}$$

$$f''(x) = \left(\frac{\pi}{L}\right)\sum_{n=1}^{\infty} n\left[\frac{2}{L}\left\{f_0 - (-1)^n f_L\right\} - \frac{\pi}{L}n a_n\right]$$

$$\times \sin\frac{n\pi x}{L}, \qquad 0 < x < L$$

$$f''(0) = f_0'', \qquad f(L) = f_L'',$$

Similar transformation formulas must be used to obtain the correct form of the successive derivatives of the

cosine series. For example the derivatives of the axial displacement u, are given below:

$$u(x,\theta) = \left(A_{0n} + \sum_{m=1}^{\infty} A_{mn} \cos\frac{m\pi x}{L}\right)\cos n\theta, \quad 0 \le x \le L$$

$$u_{,x} = -\left(\frac{\pi}{L}\right)\sum_{m=1}^{\infty} mA_{mn} \sin\frac{m\pi x}{L}\cos n\theta, \qquad 0 < x < L$$

$$u_{,x}(0,\theta) = -\left(\frac{\pi^2}{2L}\right)\bar{u}_0 \cos n\theta,$$

$$u_{,x}(L,\theta) = \left(\frac{\pi^2}{2L}\right)\bar{u}_L \cos n\theta,$$

$$u_{,xx} = \left(\frac{\pi}{L}\right)^2\left[\frac{\bar{u}_0+\bar{u}_L}{2} + \sum_{m=1}^{\infty}\left\{\bar{u}_0 + \bar{u}_L(-1)^m - m^2 A_{mn}\right\} \times \cos\frac{m\pi x}{L}\right]\cos n\theta, \qquad 0 \le x \le L$$

APPENDIX B

$$K_{11} = RA_{11}\left(\frac{m\pi}{L}\right)^2 + A_{66}\frac{n^2}{R}$$

$$K_{12} = -\left(A_{12} + A_{66} + \frac{B_{12}}{R} + \frac{B_{66}}{2R}\right)\left(\frac{mn\pi}{L}\right)$$

$$K_{13} = -A_{12}\left(\frac{m\pi}{L}\right) - RB_{11}\left(\frac{m\pi}{L}\right)^3 + (B_{12} - B_{66})\left(\frac{m\pi n^2}{RL}\right)$$

$$K_{22} = \left(RA_{66} + \frac{3B_{66}}{2} + \frac{D_{66}}{2R}\right)\left(\frac{m\pi}{L}\right)^2 + (RA_{22} + 2B_{22} + \frac{D_{22}}{R})\left(\frac{n}{R}\right)^2$$

$$K_{33} = \left(\frac{m\pi}{L}\right)^2\left(2B_{12} + RD_{11}(\frac{m\pi}{L})^2 + 2\frac{D_{12}+D_{66}}{R}n^2\right) + 2B_{22}(\frac{n}{R})^2 + \frac{A_{22}}{R} + D_{22}\frac{n^4}{R^3}$$

$$K_{01} = A_{66}\frac{n^2}{R}$$

REFERENCES

1. Yamanouchi M., Koizumi M., Hirai T. and Shiota I., *Proceedings of the First International Symposium on Functionally Gradient Materials*, (1990).
2. Koizumi M., "The Concept of FGM, Ceramic Transactions", *Functionally Gradient Materials*, **34**, PP 3-10(1993).
3. Miyamoto Y., Kaysser W. A., Rabin B. H., Kawasaki A. and Ford R. G., *Functionally Graded Materials: Design, Processing and Applications*, Kulwer Academic Publishers, London, (1990).
4. Moya J.S., "Layered Ceramics", *Advanced Materials*, **7**, PP 185-9(1995).
5. Leissa A.W., "Vibration of shells", *NASA SP- 288 US Govt Printing Office*, (1973).
6. Vanderpool M. E. V. and BERT C. W., "Vibration of Materially Monoclinic, Thick –Wall Circular Cylindrical Shells", *AIAA journal*, **19**, PP 634-641(1981).
7. Lan K.Y. and Loy C.T., "Influence of Boundary Conditions and Fiber Orientation and the Natural Frequencies of Thin Orthotropic Laminated Cylindrical Shells", *Composite Structures*, **31**, PP 21-30(1995).
8. Sharma C. B., Darvizeh M. and Darvizeh A., "Natural Frequency Response of Vertical Cantilever Composite Shells Containing Fluid", *Engineering Structures*, **20**(8), PP 732-737(1998).
9. Sharma C. B., Darvizeh M. and Darvizeh A., "Free Vibration Behaviour of Helically Wound Cylindrical Shells", *Composite Structures*, **44**, PP 55-62(1999).
10. Loy C. T., Lam K. Y. and Reddy J. N., "Vibration of Functionally Graded Cylindrical Shells", *International Journal of Mechanical Sciences*, **41**, PP 309-324(1999).
11. Pradhan S. C., Loy C. T., Lam K. Y. and Reddy J. N., "Vibration Characteristics of Functionally Graded Cylindrical Shells Under Various Boundary Conditions", *Applied Acoustics*, **61**, PP 111-129(2000).
12. Naeem M. N., "Prediction of Natural Frequencies for Functionally Graded Cylindrical Shells", PHD thesis, (2004).
13. Patel B.P., Gupta S.S., Loknath M.S., Kadu C.P., "Free Vibration Analysis of Functionally Graded Elliptical Cylindrical Shells Using Higher Order Theory", *Composite Structures*, **69**, PP 259-270(2005).
14. Ansari R., Darvizeh M., "Prediction of Dynamic Behaviour of FGM Shells Under Arbitrary Boundary Conditions", *Journal of Composite Structures, Accepted for Publication*, **10**, (2007).
15. Sanders J. L., "An Improved First Approximation Theory for Thin Shells", *NASA Report 24*, (1959).
16. Chi S.H., and Chung Y.L., "Mechanical Behavior of Functionally Graded Material Plates Under Transverse Load-Part I: Analysis", *International Journal of Solids and Structures*, **43**, PP 3657-3674(2006).
17. Chi S.H., and Chung Y.L., "Mechanical Behavior of Functionally Graded Material Plates Under Transverse Load-Part II: Numerical Results", *International Journal of Solids and Structures*, **43**, PP 3657-3691(2006).
18. Touloukian Y.S., *Thermophysical Properties of High Temperature Solid Materials*, New York, Macmillian, (1967).
19. Darvizeh M., Darvizeh A., Ansari R. Sharma C.B., "The Effect of Radius Variation on Buckling of Fibrous Composite Structures Subjected to Different Types of Loading", *Iranian Journal of Science & Technology. Transaction B*, **27**(B3), PP 535-550(2003).
20. Darvizeh M., Haftchenari H., Darvizeh A., Ansari R. and Sharma C.B., "The Effect of Boundary Conditions on the Dynamic Stability of Orthotropic Cylinders Using a Modified Exact Analysis", *Journal of Composite Structures*, **74**, PP 495-502(2006).

21. Chung H., "Free Vibration Analysis of Circular Cylinderical Shells", *Journal of Sounds & Vibration*, **74**(3), PP 331-350(1981).

22. Sewall J. L. and Naumann E. C., "An Experimental and Analytical Vibration Study of Thin Cylindrical Shells with and without Longitudinal Stiffeners", *NASA TN D-4705*, (1968).

23. Sharma C. B., "Calculation of Natural Frequencies of Fixed-Free Circular Cylindrical Shells", *Journal of Sounds & Vibration*, **35**(1), PP 55-76(1974).